Supplemental materials

Supplemental Table 1. The integrated forms of stability functions for momentum Ψ_M in the five algorithms. x and x_0 are defined as $x = (1 - \gamma_m \zeta)^{1/4}$ and $x_0 = (1 - \gamma_m \zeta_0)^{1/4}$, respectively.

Algorithm name	Ψ_M		
	Unstable (ζ <0)	Weakly stable (0<ζ <1)	Strongly stable (ζ>1)
LS87	$2ln\left(\frac{1+x^2}{1+x_0^2}\right) - 2(\text{atan}(x^2) - \text{atan}\,(x_0^2))$, $\gamma_m = 15$ (Businger et al., 1971)	$-4.7(\zeta - \zeta_0)$ (Holtslag et al., 1990)	$-4.7(1 - \zeta_0 + ln\zeta)$ (Holtslag et al., 1990)
C89	$2ln\left(\frac{1+x}{2}\right) + ln\left(\frac{1+x^2}{2}\right) - 2\,\text{atan}(x^2) + \frac{\pi}{2}$, $\gamma_m = 16$ (Businger et al., 1971)	-5.2ζ (Holtslag et al., 1990)	$-5.2(1 + ln\zeta)$ (Holtslag et al., 1990)
Z98L		-5ζ (Holtslag et al., 1990)	$-4ln\zeta + 5\zeta_0 - \zeta - 4$ (Holtslag et al., 1990)
J99		$-[0.7\zeta + 0.75(\zeta - 14.3)\exp(-0.35\zeta) + 10.7]$ (Beljaars and Holtslag, 1991)	
COARE	$\Psi_k = \frac{\Psi_k + \zeta^2\Psi_c}{1 + \zeta^2}$ $\Psi_k = 2ln\left(\frac{1+x}{2}\right) + ln\left(\frac{1+x^2}{2}\right) - 2\,\text{atan}(x^2) + \frac{\pi}{2}$ (Businger et al., 1971), $\gamma_m = 15$ Convective behavior: $\Psi_c = 1.5ln\left(\frac{1+x_c+x_c^2}{2}\right) + \sqrt{3}atan\left(\frac{1+2x_c}{\sqrt{3}}\right) + \frac{2\pi}{\sqrt{3}}$, $x_0 = (1 - \gamma_{cm}\zeta_0)^{1/3}$, $\gamma_{cm} = 10.15$ (Fairall et al., 1996)	$-\left[(1 + \zeta) + \frac{2}{3}(\zeta - 14.28)\exp(-0.35\zeta) + 8.525\right]$ (Beljaars and Holtslag, 1991)	

Supplemental Table 2. The integrated forms of stability functions for temperature and humidity $\Psi_{\theta,q}$ in the five algorithms. x and x_0 are defined as $x = (1-\gamma_h\zeta)^{1/4}$ and $x_0 = (1-\gamma_h\zeta_0)^{1/4}$, respectively.

Algorithm name	$\Psi_{\theta,q}$		
	Unstable (ζ<0)	Weakly stable (0< ζ <1)	Strongly stable (ζ >1)
LS87	$2ln\left(\frac{1+x^2}{1+x_0^2}\right)$, $\gamma_h = 9$ (Businger et al., 1971)	$-4.7Pr^{-1}(\zeta-\zeta_0)$ (Holtslag et al., 1990)	$-4.7Pr^{-1}(1-\zeta_0+ln\zeta)$ (Holtslag et al., 1990)
C89	$2ln\left(\frac{1+x^2}{2}\right)$ $\gamma_h = 16$ (Businger et al., 1971)	-5.2ζ (Holtslag et al., 1990)	$-5.2(1+ln\zeta)$ (Holtslag et al., 1990)
Z98L		$-5(\zeta-\zeta_0)$ (Holtslag et al., 1990)	$-4ln\zeta+5\zeta_0-\zeta-4$ (Holtslag et al., 1990)
J99		$-[0.7\zeta+0.75(\zeta-14.3)\exp(-0.35\zeta)+10.7]$ (Beljaars and Holtslag, 1991)	
COARE	$\Psi_k = \frac{\Psi_k+\zeta^2\Psi_c}{1+\zeta^2}$ $\Psi_k = 2ln\left(\frac{1+x^2}{2}\right)$ (Businger et al., 1971), Convective behavior: $\Psi_c = 1.5ln\left(\frac{1+x_c+x_c^2}{2}\right)+\sqrt{3}atan\left(\frac{1+2x_c}{\sqrt{3}}\right)+\frac{2\pi}{\sqrt{3}}$, $x_0 = (1-\gamma_{ch}\zeta_0)^{1/3}$, $\gamma_{ch} = 34.15$ (Fairall et al., 1996)	$-\left[(1+\frac{2}{3}\zeta)^{1.5}+\frac{2}{3}(\zeta-14.28)\exp(-0.35\zeta)+8.525\right]$ (Beljaars and Holtslag, 1991)	

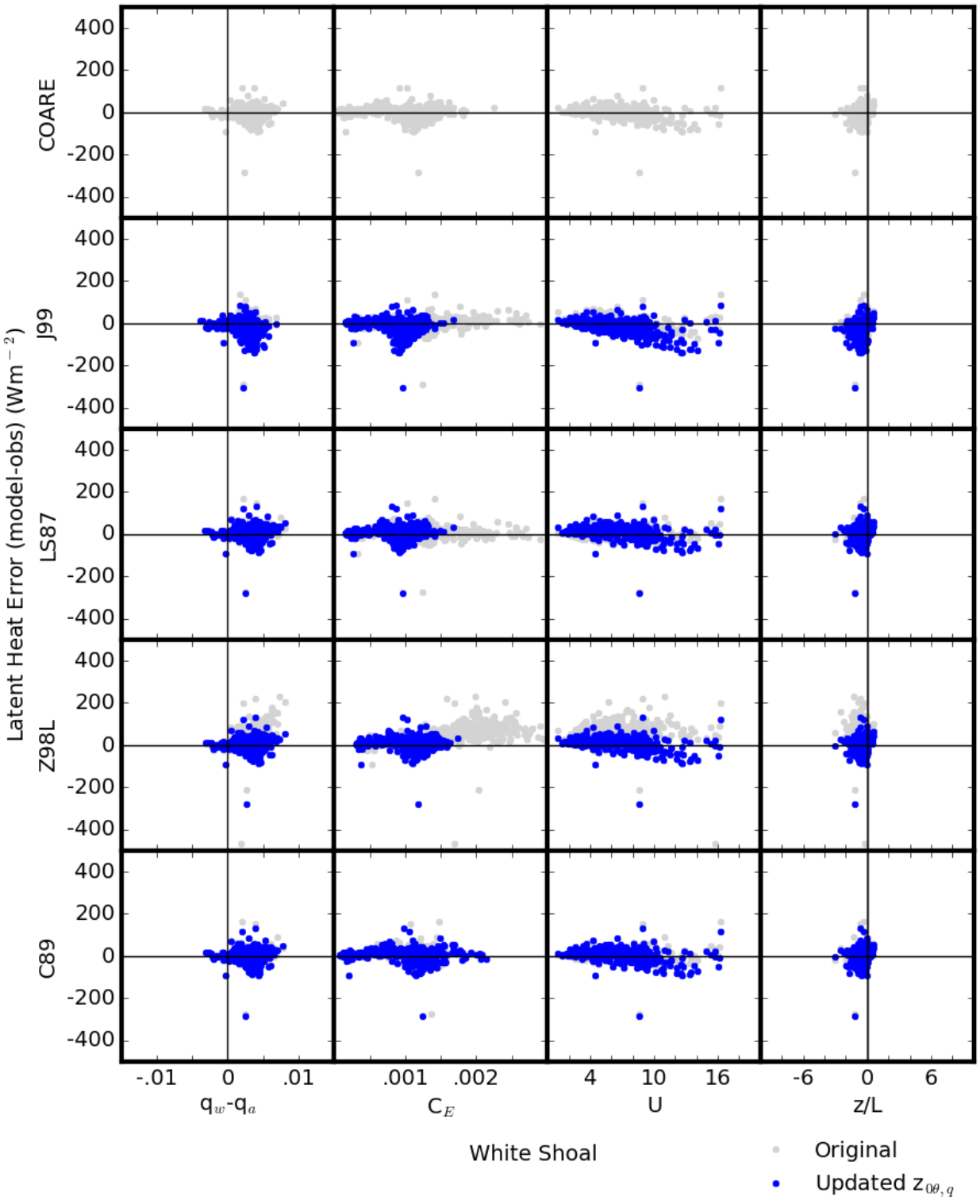

Figure S1. Errors of latent heat flux (*y*-axis) versus specific humidity difference between water surface and air at the sensor height q_w-q_a [kg kg^{-1}], transfer coefficient C_E [-], wind speed U [m s^{-1}], and stability factor z/L (*x*-axis) for the five algorithms at White Shoal. Each dot represents a daily mean value. Grey and blue dots indicate the results with the original and updated z_{0q} formulae, respectively.

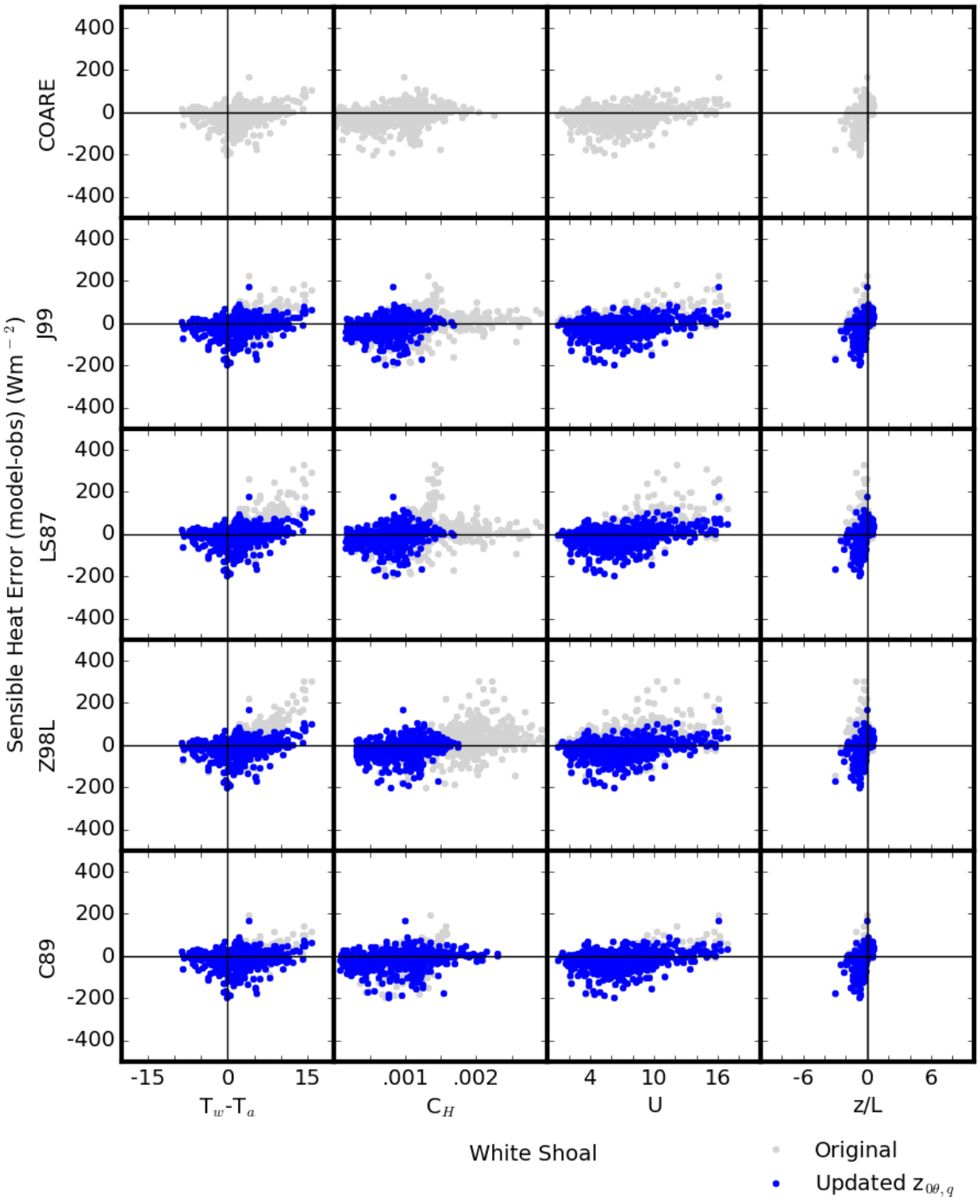

Figure S2. Errors of sensible heat flux (*y*-axis) versus temperature difference between water surface and air at the sensor height θ_w-θ_a [^{o}C], transfer coefficient C_H [-], wind speed U (m/s), and stability factor z/L (*x*-axis) for the five algorithms at White Shoal. Each dot represents a daily mean value. Grey and blue dots indicate the results with the original and updated $z_{0\theta}$ formulae, respectively.

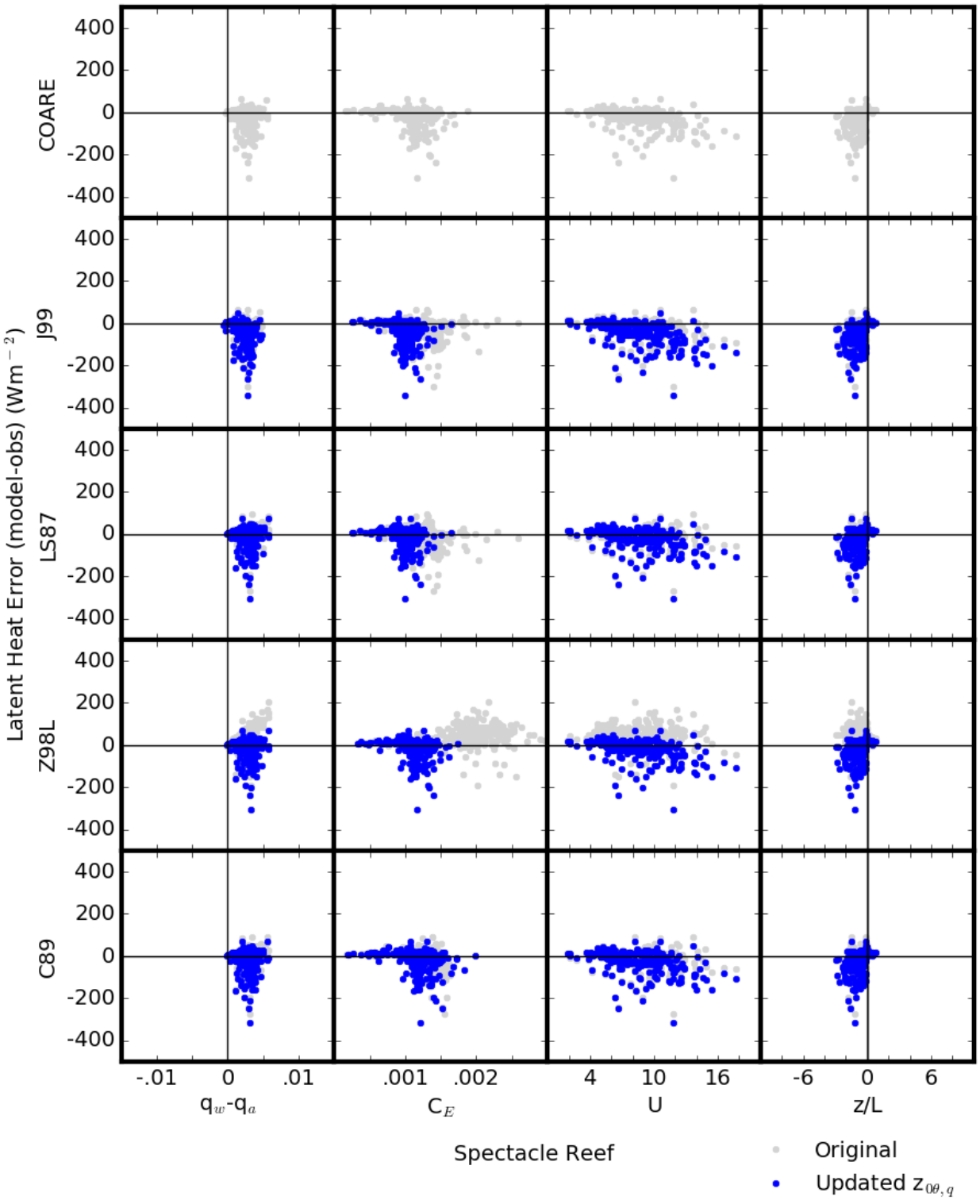

Figure S3. Similar to Fig. S1, but at Spectacle Reef.

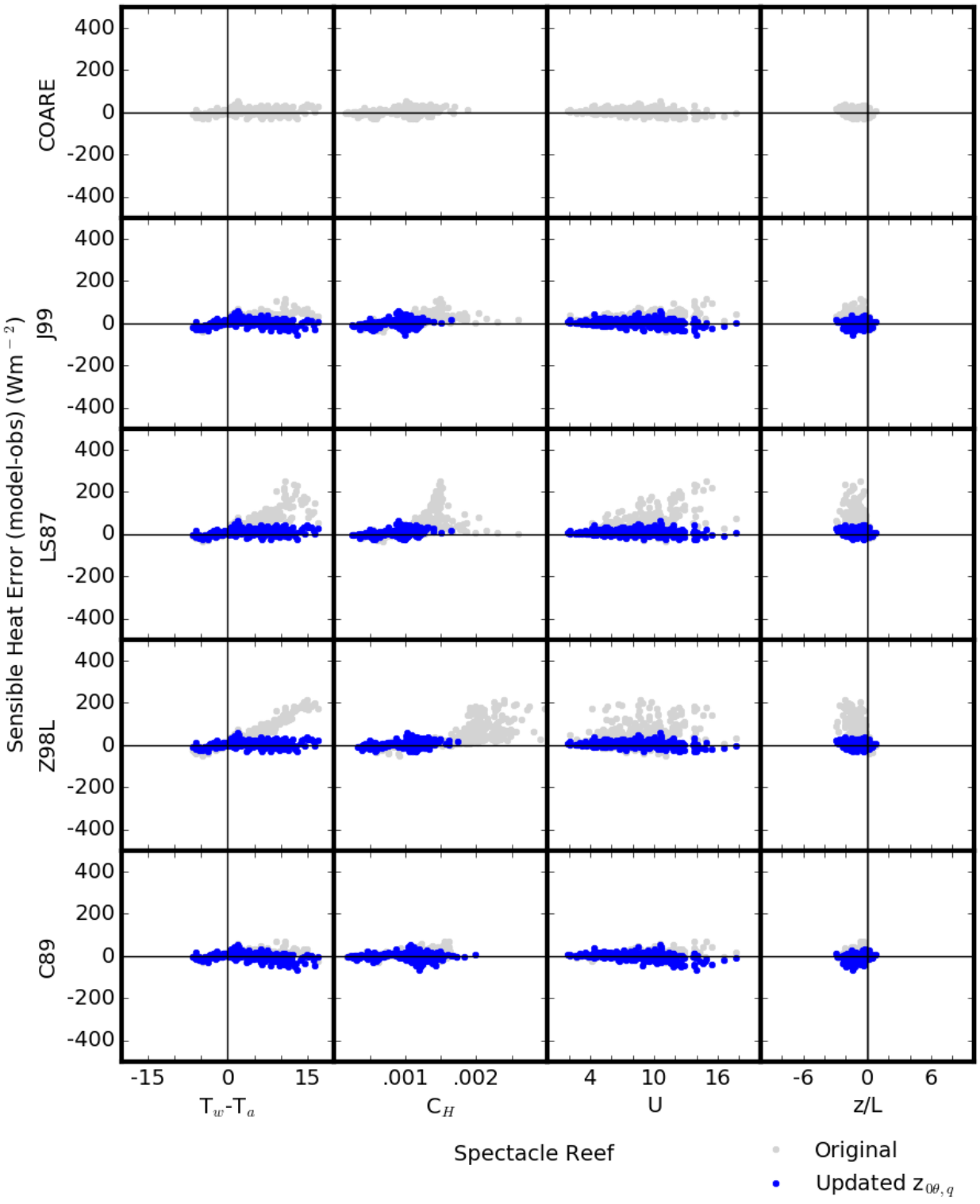

Figure S4. Similar to Fig. S2, but at Spectacle Reef.

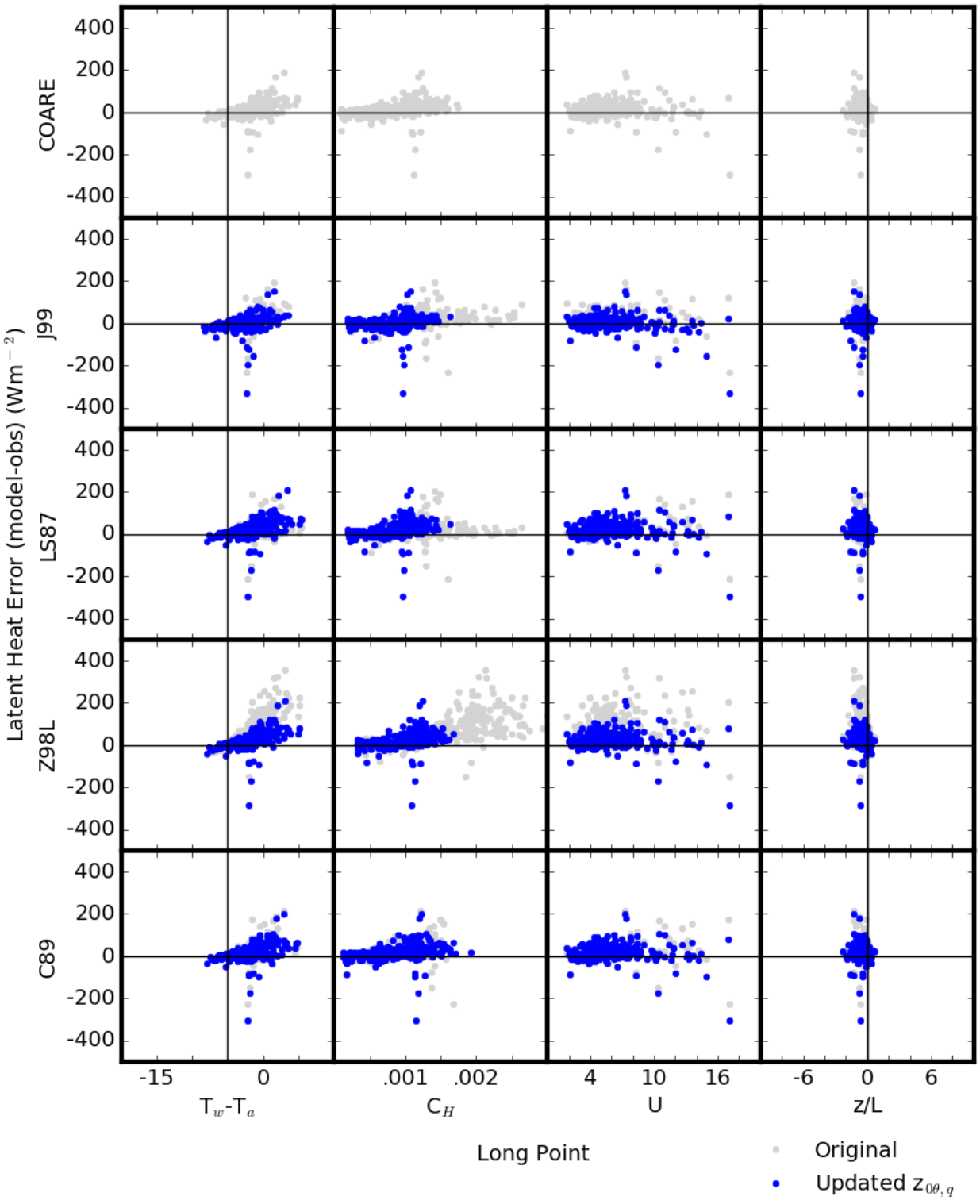

Figure S5. Similar to Fig. S1, but at Long Point.

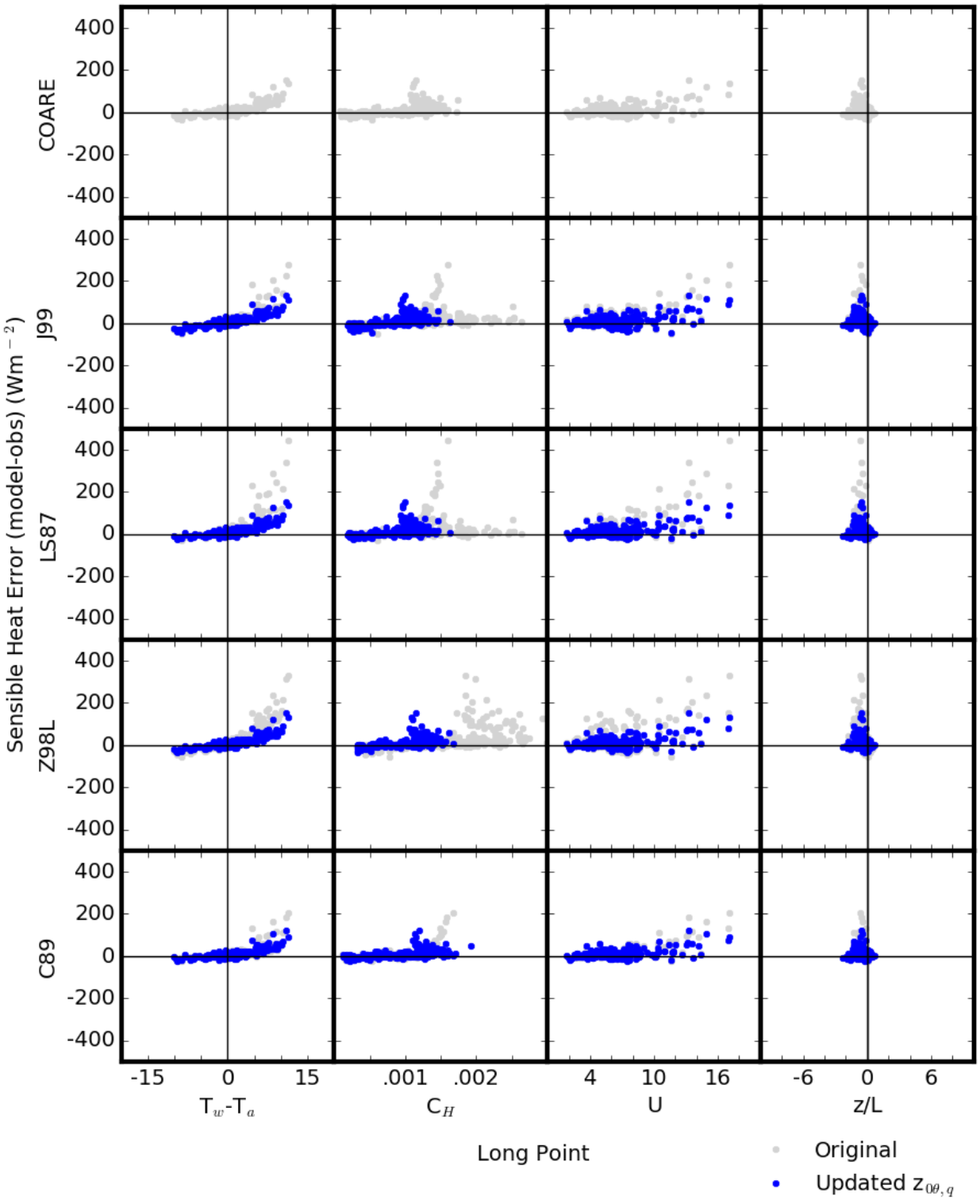

Figure S6. Similar to Fig. S2, but at Long Point.

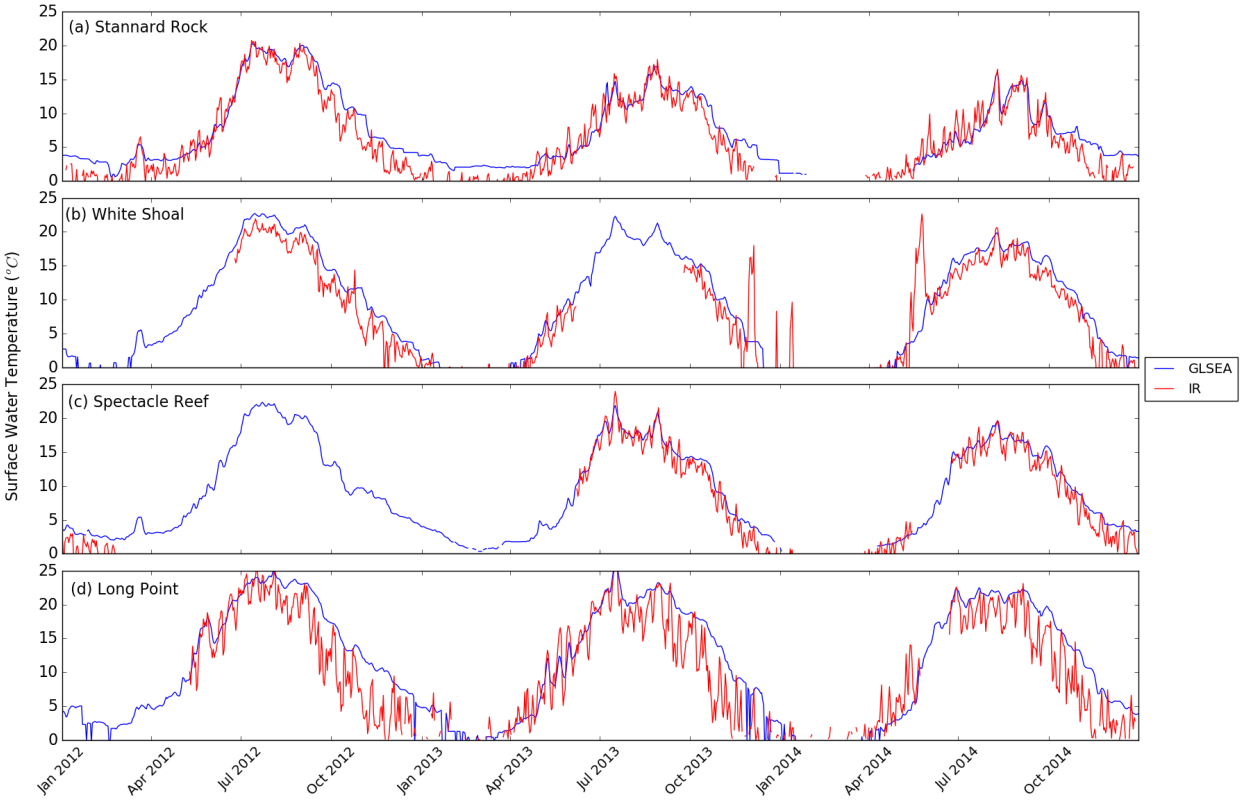

Figure S7. Daily water surface temperature at the four stations from GLSEA and Infrared thermometers (IRTs, Apogee IRR-T). For GLSEA, the closest pixel to each of the four stations was chosen. Values below zero are masked out.